



Design of Radar-Communication Integrated Signal Based on OFDM

Tianqi Liang¹(✉), Zhuoming Li^{1,2}, Mengqi Wang¹, and Xiaojie Fang¹

¹ School of Electronics and Information Engineering,
Harbin Institute of Technology, Harbin, China
1418816805@qq.com, zhuoming@hit.edu.cn
² Peng Cheng Laboratory, Shenzhen 518000, China

Abstract. With the development of information technology, the electromagnetic environment is becoming more and more complex, and the demand for bringing together electronic devices of different functions is urgently increasing. Among them, the radar-communication integration is a research hotspot. The current radar-communication integration research mainly focuses on the integrated signal design. Due to the similarity between OFDM signals and phase-encoding radars, it is possible to apply OFDM to radar. Aiming at the problem that the randomness of communication data affects the detection capability of OFDM radar, this paper proposes an integrated OFDM radar-communication signal design based on P4 cyclic shift code. And we verified communication BER and radar range and velocity performance for multi-target of the integrated system. The transmitting end carries out an integrated signal design that is consistent with the communication OFDM signal. The degree of system integration is high, and it achieves communication functions without reducing radar detection capability. For the high PAPR problem, we introduce CE-OFDM signals, and derive a radar signal processing algorithm based on FFT demodulation. This paper provides a theoretical basis for applications of OFDM-based integrated signals and it is an effective integrated scheme.

Keywords: Radar-communication integration · OFDM · P4 code · CE-OFDM

1 Introduction

The development of modern science has enriched various electronic devices but has also caused increasingly complex electromagnetic environment. Electronic equipment brings serious electromagnetic interference to each other, and the maintenance of equipment is also more time-consuming and labor-intensive. In this background, the integrated design of electronic equipment is very necessary. The high degree of similarity between the hardware of the radar equipment and the communication equipment and the sharing of software resources have brought an opportunity to the integrated design of the radar-communication [1]. Among them, the application of OFDM signals to radar for integrated shared waveform design is an option.

Shi et al. proposed three different robust radar waveform design standards based on power minimization [2, 3]. Sit et al. proposed a MIMO-OFDM joint radar-communication system and proposed a system-level interference cancellation algorithm [4]. Herschfelt and Bliss develop and simulate a joint system for a sample multiple access channel [5]. Dokhanchi et al. use phase-modulated continuous wave (PMCW) waveform to modulate a communication stream and effect of joint radar-communication system (JRC) [6]. And they design a vehicle JRC system [7]. Xu et al. introduced FBMC technology into the integrated system, and proposed an m-sequence filter bank multi-carrier (MS-FBMC) integrated radar-communication signal based on m-sequence precoding [8]. The above references don't solve the impact of randomness of communication data on radar detection capability.

Aiming at the influence of randomness of communication data on OFDM detection capability, this paper designs a OFDM radar-communication integrated signal design based on P4 cyclic shift code. This paper discusses the ambiguity function, PAPR, and reception algorithm of the integrated signal. At the same time, it introduced CE-OFDM to solve the problem of excessive PAPR. Through simulation analysis, we discuss the velocity resolution and range resolution of the radar system, the bit error rate of the communication system, and verify the rationality of the integrated signal proposed in this paper.

2 Analysis of Radar-Communication Integration Based on OFDM Signal

In this chapter, we combine the waveform design theory of radar signals, and propose the design criteria of shared waveforms. At the same time, we give a schematic diagram of the system based on OFDM radar-communication integration, and introduce its working principle. It provides guidance for theoretical derivation and simulation analysis.

2.1 Radar Waveform Design Guidelines

The guidelines for measuring the detection capability of radar signals are mainly ambiguity function and interception factors. The output of the radar signal through the matched filter is given by

$$\begin{aligned} y(t; F_D) &= \int_{-\infty}^{+\infty} x(s) \exp(j2\pi F_D s) x^*(s-t) ds \\ &= \hat{A}(t, F_D) \end{aligned} \quad (1)$$

We consider the output of the matched filter with the waveform $x(t)$ when the input is a Doppler shift response $x(t)\exp(j2\pi F_D t)$. We assume that the filter has unity gain and is designed to peak at zero. A fuzzy function can be defined as

$$A(t, F_D) = |\hat{A}(t, F_D)| \quad (2)$$

By analyzing the ambiguity function, we can evaluate the detection capabilities of radar signals, such as resolution, side lobe performance, and Doppler and range ambiguity. The design should be as close as possible to the ambiguity function, which is characterized by a single central peak, while other energy is evenly distributed in the delayed Doppler plane, which can improve the target resolution.

Another important performance parameter of radar is the intercept factor. The interception factor γ is defined as the ratio of the maximum range of the radar signal that can be received by the interceptor to the maximum detected range of the intercepted radar. Obviously, the smaller the γ , the better. Moreover, γ is inversely proportional to the time-width bandwidth product. Therefore, the pulse compression radar with a large time-width and wide-band product characteristic has a low probability of interception. When designing a radar signal, the time-width bandwidth product should be set as large as possible.

2.2 System Schematic Diagram of OFDM Radar

Based on the architecture of the traditional radar-communication integrated system, this paper gives a schematic diagram of the OFDM radar-communication integrated system. It can be seen in Fig. 1.

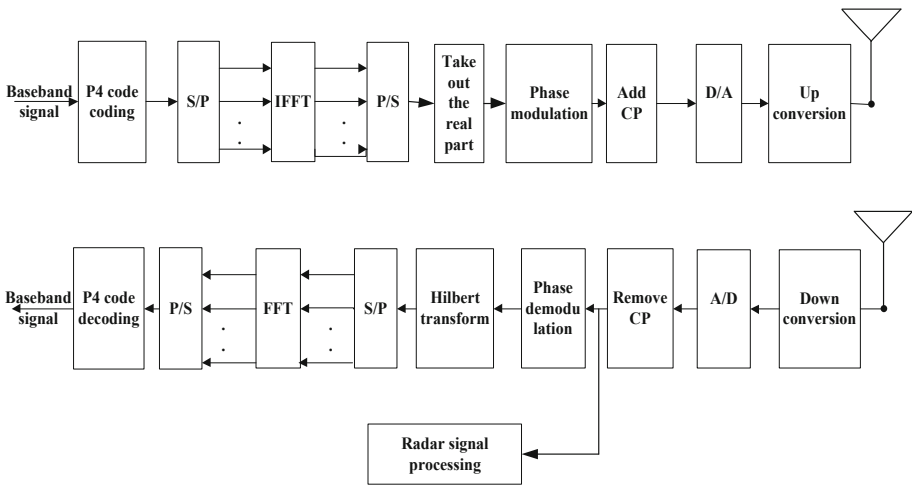


Fig. 1. The schematic diagram of the OFDM radar-communication integrated system.

The radar-communication integrated system adds a P4 code coding map based on the original OFDM system, maps the random bit data into a P4 code sequence, and uses the phase randomness of the P4 code cyclic shift sequence to represent the data information. The receiving end adds a radar signal processing module, which adopts an FFT demodulation receiving algorithm, and the communication part adopts a conventional OFDM demodulation algorithm. The whole system uses software radio technology, so the hardware part before the A/D converter is shared, and the radar signal processing function will be realized by software, and the degree of integration is very high.

3 OFDM Shared Signal Waveform Design

Based on the above system schematic diagram, we derive and simulate the OFDM shared signal waveform. Based on the derivation of the fuzzy function of OFDM signal, it introduces the P4 cyclic code to simulate the ambiguity function, and proposes the CE-OFDM method to reduce PAPR, and analyzes its influence on the ambiguity function.

3.1 Ambiguity Function of OFDM Signal

The signal design of this paper starts from the classical OFDM signal, and its transmitted signal form is given by

$$s(t) = \text{rect}(t) \sum_{k=0}^{N-1} C_k \exp\{j2\pi(k\Delta f + f_c)t\} \quad (3)$$

where $\text{rect}(t)$ is a window function, N is the number of subcarriers, C_k is the subcarrier amplitude, Δf is the carrier spacing, f_c is the carrier frequency.

When the signal encounters a target with a distance of R and a relative radar radial velocity of v , the echo signal received by the receiver is given by

$$r(t) = \text{rect}(t\gamma - \tau) \sum_{l=0}^{N-1} C_l \exp\{j2\pi(l\Delta f + f_c)(t\gamma - \tau)\} \quad (4)$$

where γ is the stretching factor, τ is the delay, and c is the speed of light. The echo signal is down-converted to obtain the baseband signal and brought into the ambiguity function formula simplification. Due to the orthogonality of the subcarriers, we take the main part of the energy to get

$$\begin{aligned} \chi_M(\tau, f_d) = & \exp\{j2\pi f_c \tau\} \sum_{k=0}^{N-1} \exp\{j2\pi k \Delta f \tau\} C_k C_k^* \\ & \sin c(\pi(f_c - k\Delta f)(1 - \gamma)T_d) \\ & \exp\{j\pi(f_c - k\Delta f)(\gamma - 1)T_a\} \end{aligned} \quad (5)$$

where $T_d = T_{\max} - T_{\min}$, $T_a = (T_{\max} - T_{\min})/2$, $T_{\min} = \max(0, \tau)$, $T_{\max} = \min(T_s, T_s/\gamma + \tau)$.

When $\tau = 0$, $f_d = 0$, ambiguity function reaches the maximum; $\tau \neq 0$, $f_d = 0$, ambiguity function becomes range ambiguity function; $\tau = 0$, $f_d \neq 0$, ambiguity function becomes velocity ambiguity function. Range resolution is inversely proportional to bandwidth, and we can obtain the combined high resolution of range and Doppler by pulse compression.

3.2 Design of OFDM Shared Signal Based on P4 Complementary Code

Since the signal and echo forms given above cannot carry random information, we introduce the P4 code commonly used in radar. The P4 code is defined as

$$\phi_m = \frac{2\pi}{M}(m-1) \frac{(m-1-M)}{2} \quad (6)$$

where M is the number of P4 code bits, and m is the current bit.

A prominent feature of the P4 code is that its cyclic shift can constitute a complementary set. The sum of the autocorrelation functions of the complementary set is a side lobe of zero and the main lobe is a function of the sum of the peaks. If the complementary code generated by cyclically shifting the P4 code is combined with the OFDM signal, the shared signal can have communication capabilities.

To this end, we chose the P4 complementary code for shared signal design. The sequential shift sequence of the P4 code can form a P4 complementary code set, taking the 4-bit P4 code as an example, and the complementary code set is given by

$$\begin{aligned} \phi_1 &= \left\{ 0, \frac{5}{4}\pi, \pi, \frac{5}{4}\pi \right\} & \phi_2 &= \left\{ \frac{5}{4}\pi, \pi, \frac{5}{4}\pi, 0 \right\} \\ \phi_3 &= \left\{ \pi, \frac{5}{4}\pi, 0, \frac{5}{4}\pi \right\} & \phi_4 &= \left\{ \frac{5}{4}\pi, 0, \frac{5}{4}\pi, \pi \right\} \end{aligned} \quad (7)$$

We can make $\phi_1 \phi_2 \phi_3 \phi_4$ represent different data information respectively, and think that the probability of occurrence of symbols is the same. Then, when the receiver performs the coherent integration processing of the pulses, the side lobes cancel each other due to the complementary code characteristics of the P4 code. Therefore, the side lobes of the ambiguity function at this time will also be very low, and the more the cumulative number of pulses, the more obvious the effect. At this point, the expression of the integrated signal is given by

$$\begin{aligned} y(n, m) &= \sum_{m=1}^M \text{rect}(t - (M-1)T_s) \sum_{k=0}^{N-1} \exp(j\varphi_{k,m}) \exp\left\{j2\pi k \frac{n}{N}\right\} \\ \varphi_{k,m} &= \frac{2\pi}{N}(k-1 + c_m - 1) \frac{(k-1 - N + c_m - 1)}{2} \\ c_m &\in \{1, 2, 3, \dots, N\} \end{aligned} \quad (8)$$

where each OFDM chip signal represents a communication symbol, and c_m is a sequence number representing a communication symbol obtained by bit mapping of the data information. The phase modulated on each subcarrier in each chip signal is determined by the equations of the c_m and P4 codes, and c_m determines the shift of the modulated P4 code sequence in each chip. Thus different shifts can represent different data information.

Use (5) to write the main lobe formula of the ambiguity function

$$\chi_M(\tau, f_d) = \sum_{k=0}^{N-1} \exp\{j2\pi(f_c + k\Delta f)\tau\} \sum_{l=0}^{M-1} \sum_{m=0}^{M-1} C_{k,l} C_{k,m}^* \quad (9)$$

$$T_d \sin c(\pi(f_c - k\Delta f)(1 - \gamma)T_d)$$

$$\exp\{j\pi(f_c - k\Delta f)(\gamma - 1)T_d\}$$

where $C_{k,l}$, $C_{k,m}$ are the l th symbol and the k th symbol on the k th subcarrier in the OFDM signal, respectively. P4 code ambiguity function zero Doppler plane simulation results are shown in Fig. 2.

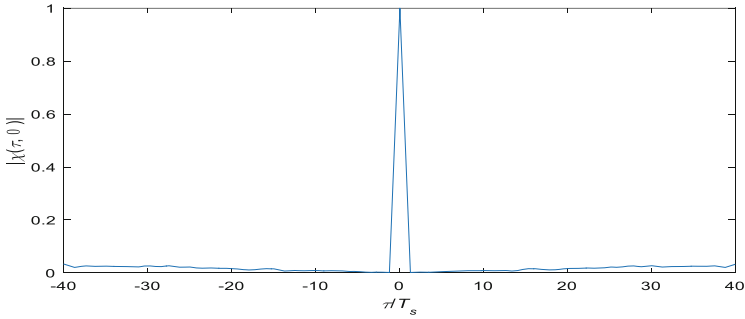


Fig. 2. Improved P4 code zero Doppler plane.

Figure 2 is a range ambiguity function obtained by accumulating 1024 pulses using a 32-bit P4 code. It can be seen that the main lobe is narrow and the side lobes are low. Therefore, the radar detection capability of the integrated signal designed by this method is hardly reduced.

3.3 Method for Reducing PAPR of Shared Signals

Too high PAPR is an unavoidable problem for OFDM systems, and integrated systems are also facing this problem. The traditional clipping method has a small change to the ambiguity function due to the clipping ratio (CR), but has a great influence on BER. To this end, we introduce CE-OFDM to solve the problem of excessive PAPR.

The CE-OFDM method combines OFDM technology with angle modulation or frequency modulation to produce a constant envelope signal that allows the amplifier to operate in saturation and maximize energy efficiency. The PAPR of the signal can be as high as 0 dB. For the sake of discussion, let's take angle modulation as an example. In the CE-OFDM-PM signal, the angle signal should be proportional to the real part of the OFDM signal. We construct the real OFDM signal and combine the angle modulation to obtain the formula of the CE-OFDM-PM signal. It is given by

$$y(t) = A \exp \left(jh_p \sum_{n=1}^{2N} \left\{ \Re[X(n)] \cos \left(j2\pi \frac{n}{T_s} t \right) - \Im[X(n)] \sin \left(j2\pi \frac{n}{T_s} t \right) \right\} \right) \quad (10)$$

where h_p is the angle modulation index, and T_s is the OFDM symbol duration, which is reciprocal with the subcarrier spacing to ensure orthogonality.

In the echo signal of the CE-OFDM-PM signal, the effects of delay and Doppler shift will all be applied to the angle signal, so the ambiguity function of CE-OFDM is exactly the same as the ambiguity function of OFDM signal above. The signal ambiguity function simulation results are shown in Fig. 3.

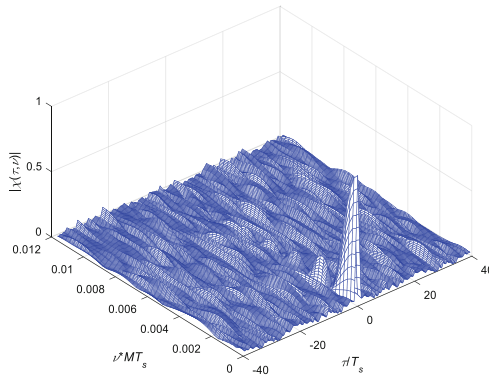


Fig. 3. Ambiguity function graph of CE-OFDM signal modulated by P4 code.

It can be seen that the side lobes are undulating, but not very prominent, and the width of the main lobe is narrow. Therefore, the CE-OFDM signal can be considered as a suitable radar detection signal, which can be directly subjected to pulse compression processing. However, the disadvantage of this method is that the angle demodulation has a threshold effect, which requires that the SNR of the demodulator is greater than 10 dB, which will affect the detection range of the radar.

4 Design and Simulation Analysis of OFDM Integrated Signal Reception Algorithm

4.1 OFDM Integrated Signal Receiving Algorithm Based on FFT Demodulation

Taking a single pulse signal as an example, after down-conversion, A/D conversion, phase demodulation, and Hilbert transform, the expression of the baseband signal entering the radar processing module is given by

$$\begin{aligned}
s(n) = & \text{rect}\left(\frac{n}{N\Delta f}\left(1 - \frac{2v}{c}\right) - \tau\right) \sum_{m=0}^{N-1} [\exp(j\varphi_m) \\
& \exp\left\{j2\pi m\Delta f \frac{n}{N\Delta f}\left(1 - \frac{2v}{c}\right)\right\} \\
& \exp\left\{-j2\pi f_c \frac{n}{N\Delta f} \frac{2v}{c}\right\} \\
& \exp\left\{-j2\pi(f_c + m\Delta f) \frac{n}{N\Delta f} \frac{2R}{c}\right\}]
\end{aligned} \tag{11}$$

where n is the number of samples, and the other parameters have the same meaning as above. If the above formula is rewritten as a matrix, the sampled data before entering the radar signal processing module is given by

$$\mathbf{s} = \psi \xi \mathbf{\beta} (\mathbf{a} \otimes \boldsymbol{\varphi}) \tag{12}$$

The meaning of each parameter is as follows

$$\psi = \exp\left\{-j2\pi f_c \frac{2R}{c}\right\} \tag{13}$$

$$\xi = \text{diag}\{1 \quad \gamma \quad \gamma^2 \quad \dots \quad \gamma^{N-1}\} \tag{14}$$

$$\mathbf{\beta} = \begin{bmatrix} 1 & 1 & 1 & \dots & 1 \\ 1 & \beta & \beta^2 & & \beta^{N-1} \\ 1 & \beta^2 & \beta^4 & & \beta^{2(N-1)} \\ & & & \ddots & \vdots \\ 1 & \beta^{N-1} & \beta^{2(N-1)} & \dots & \beta^{(N-1)^2} \end{bmatrix} \tag{15}$$

$$\mathbf{a}^T = [1 \quad a \quad a^2 \quad \dots \quad a^{N-1}] \tag{16}$$

$$\boldsymbol{\varphi}^T = [\exp\{j\varphi_0\} \quad \exp\{j\varphi_1\} \quad \dots \quad \exp\{j\varphi_{N-1}\}] \tag{17}$$

The derivation of the range output and velocity output of the formula is summarized as the following algorithm:

- Step 1: Each pulse is down-converted, sampled, and demodulated data is stored in a matrix S , and each column of the matrix represents a pulse.
- Step 2: Multiply each column in the matrix S by the Hadamard multiplication by the corresponding transmission data, and store the result in the original position.
- Step 3: Perform an IFFT transformation on each column of the matrix S , and store the result in the original position, and the result is a range output.
- Step 4: Perform FFT transformation on each row of the matrix S , and the result is the speed output.

4.2 Integrated System Simulation and Performance Analysis for Reducing PAPR of Shared Signals

Based on the above shared signal design, we simulated the integrated system, and the system parameter settings are shown in Table 1.

Table 1. System parameter setting.

Symbol	Parameter	Value
B	Bandwidth	6.4 MHz
N	Number of subcarriers	16
Δf	Carrier spacing	400 kHz
T_s	Symbol duration	2.5 μ s
M	Number of pulse	1024
T_{PRI}	Pulse repetition time	3.125 μ s
f_c	Carrier frequency	10 GHz
δR	Range resolution	25 m
δv	Velocity resolution	4.7 m/s

Suppose the radar scattering area of two targets is 1 m^2 , their distance from the radar is 100 m and 200 m, respectively, and their velocity is 200 m/s and 300 m/s. The range output and velocity output are shown in Fig. 4.

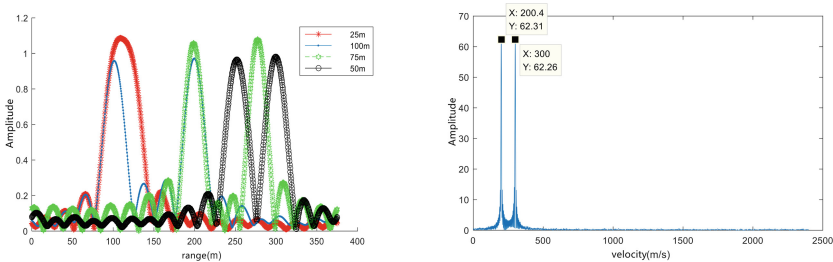


Fig. 4. Radar detection capability simulation results. Among them, the left figure shows the range output of the radar, and the right figure shows the velocity output of the radar.

It can be seen from the figure that the velocity and range of the two targets can be accurately distinguished, and the amplitude attenuation caused by the Doppler shift hardly affects the target recognition. The left image also shows the range display of the radar with two targets separated by 25 m, 50 m and 75 m. It is apparent from the figure that the two targets are indistinguishable when they are separated by 25 m. In the case of 50 m and 75 m, it is still distinguishable.

Using the system parameter, to achieve a Doppler shift of Δf , the target's velocity of motion should be 2500 m/s. We assume that the target position is 100 m and the

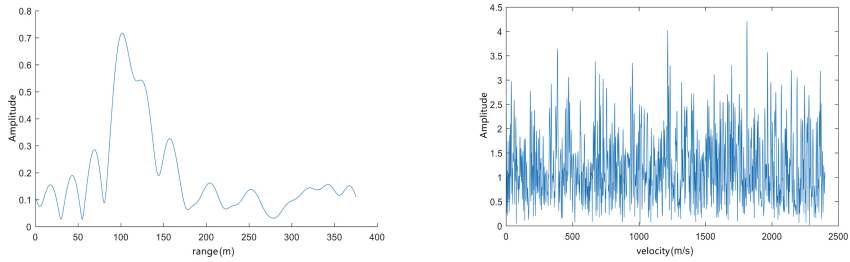


Fig. 5. Simulation results of radar detection capability under large Doppler shift. Among them, the left figure shows the range output of the radar, and the right figure shows the velocity output of the radar.

velocity is 2500 m/s, so the range output and velocity output at this time are shown in Fig. 5.

It can be seen that the range output has a very high secondary peak at 125 m, and the velocity is completely indistinguishable.

BER of CE-OFDM systems. We assume that the channel is a constant reference channel and the noise is white Gaussian noise. Considering the frequency offset produced by the channel, the signal will produce an additional phase after entering the angle demodulator. Due to the orthogonality and periodicity of the carrier, the problem of the symbol error rate of the CE-OFDM system can be reduced to the problem of the symbol error rate of the portion related to the number of bits of P4 cyclic code [11].

Using above analysis, we use the 16-bit P4 code to simulate the system BER based on the original parameters. The result is shown in Fig. 6.

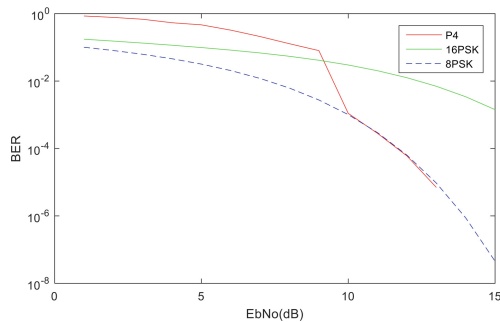


Fig. 6. BER under 16-bit P4 code white Gaussian noise channel.

As can be seen from the figure, due to the threshold effect of the angle modulation, the BER is high before the SNR is 10 dB. Under high SNR conditions, the BER of the design signal is close to the BER of 8PSK, and there is no loss in communication performance.

5 Conclusion

Aiming at the difficulty of the influence of communication data correlation on radar detection capability in radar-communication integrated signal design, this paper constructs shared signal with P4 cyclic code and CE-OFDM. And it is based on the basic theory of ambiguity function of radar signal and the waveform characteristics of OFDM. In this way, we solved the impact of relevance. At the same time, we deduced the integrated receiving algorithm based on FFT demodulation and simulated the corresponding radar range and velocity detection capability and communication BER, and obtained good results.

The radar-communication integrated system based on OFDM signal not only reduces the performance of the radar system, but also has the capability of high-speed communication, and the degree of integration is high, which is an effective and feasible integrated solution. It is also necessary to improve the clutter filtering and Doppler processing operations of the radar receiving algorithm in this system, so that the integrated system has better performance. Moreover, we need to improve the application of this radar-communication integrated system in SAR radar in the follow-up work.

References

1. Chen, X.B., Wang, X.M., Cao, C. (eds.): *Techniques Analysis of Radar-Communication Integrating Waveform*. China Academy of Electronics and Information Technology, Beijing, China (2013)
2. Garmatyuk, D., Schuerger, J., Kauffman, K.: Multifunctional software-defined radar sensor and data communication system. *IEEE Sens. J.* **11**(1), 99–106 (2011)
3. Shi, C.G., Wang, F., Sellathurai, M.: Power minimization-based robust OFDM radar waveform design for radar and communication systems in coexistence. *IEEE Trans. Signal Process.* **66**(5), 1316–1330 (2018)
4. Chalise, B.K., Himed, B.: Dual-function radar-communication using GPS gold codes. In: *International Conference on Radar Systems (Radar 2017)* (2017)
5. Sit, Y.L., Nuss, B., Zwick, S.: On mutual interference cancellation in a MIMO OFDM multiuser radar-communication network. *IEEE Trans. Veh. Technol.* **67**(4), 3339–3348 (2018)
6. Herschfelt, A., Bliss, D.W.: Joint radar-communications waveform multiple access and synthetic aperture radar receiver. In: *2017 51st Asilomar Conference on Signals, Systems, and Computers* (2017)
7. Dokhanchi, S.H., Bhavani Shankar, M.R., Stifter, T. (eds.): OFDM-based automotive joint radar-communication system. In: *Accepted to be Presented at IEEE Radar Conference (RadarConf)*, Oklahoma, OK (2018)
8. Dokhanchi, S.H., Bhavani Shankar, M.R., Nijsure, Y.A. (eds.): Joint automotive radar-communications waveform design. In: *Proceeding IEEE International Symposium on Personal, Indoor and Mobile Radio Communications, Montreal, QC, Canada* (2017)
9. Xu, W.W., Wang, C., Cui, G.F. (eds.): The M-sequence encoding method for radar-communication system based on filter bank multi-carrier. In: *2017 9th International Conference on Advanced Infocomm Technology (ICAIT)* (2017)

10. Li, Z.Q., Mei, J.J., Hu, D.P. (eds.): *Peak-to-Average Power Ratio Reduction for Integration of Radar and Communication Systems Based on OFDM Signals with Block Golay Coding*. Air Force Early Warning Academy, Wuhan, China (2014)
11. Azurdia-Meza, C.A., Lee, K., Lee, K.: PAPR reduction by pulse shaping using Nyquist linear combination pulses. *IEICE Electron. Express* **9**(19), 1534–1541 (2012)
12. Ziemer, R.E., Tranter, W.H.: *Principles of Communications: Systems, Modulation, and Noise*. Wiley, Hoboken (2015)